

---

# Bandits with Abstention under Expert Advice

---

Stephen Pasteris<sup>1</sup> Alberto Rumi<sup>2,3</sup> Maximilian Thiessen<sup>4</sup> Shota Saito<sup>5</sup> Atsushi Miyachi<sup>2</sup> Fabio Vitale<sup>2</sup>  
Mark Herbster<sup>5</sup>

## Abstract

We study the classic problem of prediction with expert advice under bandit feedback. Our model assumes that one action, corresponding to the learner’s abstention from play, has no reward or loss on every trial. We propose the CBA algorithm, which exploits this assumption to obtain reward bounds that can significantly improve those of the classical EXP4 algorithm. We can view our problem as the aggregation of confidence-rated predictors when the learner has the option of abstention from play. Importantly, we are the first to achieve bounds on the expected cumulative reward for general confidence-rated predictors. In the special case of specialists we achieve a novel reward bound, significantly improving previous bounds of SPECIALISTEXP (treating abstention as another action). As an example application, we discuss learning unions of balls in a finite metric space. In this contextual setting, we devise an efficient implementation of CBA, reducing the runtime from quadratic to almost linear in the number of contexts. Preliminary experiments show that CBA improves over existing bandit algorithms.

## 1. Introduction

We study the classic problem of prediction with expert advice under bandit feedback. The problem is structured as a sequence of trials. During each trial, each expert recommends a probability distribution over the set of possible actions. The learner then selects an action, observes, and incurs the (potentially negative) reward associated with that action on that particular trial. In practical applications, errors often lead to severe consequences, and consistently making predictions is neither safe nor economically practical. For this reason, the abstention option has gained a lot of interest in the literature, both in the batch and online setting (Chow,

1957; 1970; Hendrickx et al., 2021; Cortes et al., 2018). Similarly to previous works, this paper is based on the assumption that one of the actions always has zero reward: such an action is equivalent to an abstention of the learner from play. Apart from the fact that the rewards are bounded, we make no further assumptions on how the rewards or expert predictions are generated. In this paper, we present an efficient algorithm CBA (**C**onfidence-rated **B**andits with **A**bstentions) which exploits the abstention action to get reward bounds that can be dramatically higher than those of EXP4 (Auer et al., 2002). In the worst case, our reward bound essentially matches that of EXP4 so that CBA can be seen as a strict improvement, since the time-complexities of the two algorithms are identical in the general case.

Our problem can also be seen as that of aggregating *confidence-rated predictors* (Blum & Mansour, 2007; Gailard et al., 2014; Luo & Schapire, 2015) when the learner has the option of abstaining from taking actions. When the problem is phrased in this way, at the start of each trial, each predictor recommends a probability distribution over the actions (which now may not include an action with zero reward) but with a confidence rating. A low confidence rating can mean that either the predictor thinks that all actions are bad (so that the learner should abstain) or simply does not know which action is the best. Previous works measure the performance of their algorithm in terms of a sum of *scaled* per-trial rewards.

In contrast to previous algorithms for confidence-rated predictors, our approach allows for the derivation of bounds on the expected cumulative reward of CBA. One specific scenario where prior algorithms can establish cumulative reward bounds is when the predictors are *specialists* (Freund et al., 1997), having either full confidence (a.k.a. *awake*) or no confidence (a.k.a. *asleep*) on any given trial. The SPECIALISTEXP algorithm, a bandit version of the standard specialist algorithm (Herbster et al., 2021), achieves regret bounds with respect to any subset of specialists in which exactly one specialist is awake on each trial. In Section 6, we present an illustrative problem involving learning balls in a space equipped with a distance function. This example demonstrates our capability to significantly outperform SPECIALISTEXP, which treats abstention as just another action, when our confidence-rated predictors are indeed specialists.

<sup>1</sup>The Alan Turing Institute, UK <sup>2</sup>CENTAI Institute, Italy  
<sup>3</sup>University of Milan, Italy <sup>4</sup>TU Wien, Austria <sup>5</sup>University College London, UK. Correspondence to: Stephen Pasteris <spasteris@turing.ac.uk>.

For this problem, we will give subroutines that significantly speed up CBA. We note that, for any specialist problem, in the worst case the cumulative reward of CBA is essentially equal to that of SPECIALISTEXP so that it can be seen as a strict improvement.

### 1.1. Additional Related Work

The non-stochastic multi-armed bandit problem, initially introduced by Auer et al. (2002), has been a subject of significant research and interest. Auer et al. (2002) also introduced the multi-armed bandit problem with expert advice, introducing the EXP4 algorithm. The EXP4 algorithm, evolved the field of traditional multi-armed bandits to encompass more complex scenarios, particularly the contextual bandit setting (Lattimore & Szepesvári, 2020). Contextual bandits represent an extension of the classical multi-armed bandit framework, where an agent makes a sequence of decisions while taking into account contextual information.

As discussed in the introduction, a key aspect of this work is the option to abstain from making any decision. In the batch setting (Chow, 1957; 1970), this is usually referred to as machine learning with “rejection”, as these works study whether to utilize or reject a specific model prediction based on the specific request (see Hendrickx et al. (2021) for a survey). This line of research translated into the online learning world with the possibility of abstention by the learner. In these works, the authors usually rely on a cost associated with the abstention action. Neu & Zhivotovskiy (2020) studied the magnitude of the cost associated with abstention in an expert setting with bounded losses. They state that if the cost is lower than half of the amplitude of the interval of the loss, it is possible to derive bounds that are independent of the time horizon. In Cortes et al. (2018) a non-contextual and partial information setting with the option of abstention is studied. The sequel model (Cortes et al., 2020) regards this model as a special case of their stochastic feedback graph model. Schreuder & Chzhen (2021) also studied the possible implication in the fairness setting when utilizing the option of abstaining as it could lead to discriminatory predictions.

Our work is also related to the multi-class classification with bandit feedback introduced as *weak reinforcement* (Auer & Long, 1999). An action in our bandit setting corresponds to a class in the multi-class classification framework.

The study most akin to ours is that of Herbster et al. (2021), which introduced the SPECIALISTEXP algorithm, a bandit variant of the standard SPECIALISTS algorithm from Freund et al. (1997). We differ from these works as the abstention is treated as an algorithmic choice, introducing a variant of the specialist framework. Instead of sleeping in the rounds where the specialist is not active, the specialist will vote for abstention, which is a proper action of our algorithm.

## 2. Problem Formulation and Notation

We consider the classic problem of prediction with expert advice under bandit feedback. In this problem we have  $K + 1$  actions,  $E$  experts, and  $T$  trials. On each trial  $t$ :

1. Each expert suggests, to the learner, a probability distribution over the  $K + 1$  actions.
2. The learner selects an action  $a_t$ .
3. The reward incurred by action  $a_t$  on trial  $t$  (which is in  $[-1, 1]$  and is selected by Nature before the trial) is revealed to the learner.

The aim of the learner is to maximize the cumulative reward obtained by its selected actions. As discussed in Section 1, we consider the case where there is an action that incurs zero reward on every trial, for the abstention action.

We denote our action set by  $[K] \cup \{\square\}$  where  $\square$  is the abstention action. For each trial  $t \in [T]$  we define the vector  $\mathbf{r}_t \in [-1, 1]^K$  such that for all  $a \in [K]$ ,  $r_{t,a}$  is the reward obtained by action  $a$  on trial  $t$ . Moreover, we define  $r_{t,\square} := 0$  which is the reward of the abstention action  $\square$ .

It will be useful for us to represent probability distributions over the actions by vectors in the set:

$$\mathcal{A} := \{\mathbf{s} \in [0, 1]^K \mid \|\mathbf{s}\|_1 \leq 1\}.$$

Any vector  $\mathbf{s} \in \mathcal{A}$  represents the probability distribution over actions which assigns, for all  $a \in [K]$ , a probability of  $s_a$  to action  $a$ , and assigns a probability of  $1 - \|\mathbf{s}\|_1$  to the abstention action  $\square$ , where  $\|\mathbf{s}\|_1$  denotes 1-norm of  $\mathbf{s}$ . We write  $a \sim \mathbf{s}$  to represent that an action  $a$  is drawn from this probability distribution. We will refer to the elements of the set  $\mathcal{A}$  as *stochastic actions*.

A *policy* is any element of  $\mathcal{A}^T$  (noting that any such policy is a matrix in  $[0, 1]^{T \times K}$ ). Any policy  $\mathbf{e} \in \mathcal{A}^T$  defines a stochastic sequence of actions: on every trial  $t \in [T]$  an action  $a \in [K] \cup \{\square\}$  being drawn as  $a \sim \mathbf{e}_t$ . Note that if the learner plays according to a policy  $\mathbf{e} \in \mathcal{A}^T$  then on each trial  $t$  it obtains an expected reward of  $\mathbf{r}_t \cdot \mathbf{e}_t$ , where the operator  $\cdot$  denotes the dot product. Note that each expert is equivalent to a policy. Thus, for all  $i \in [E]$  we denote the  $i$ -th expert by  $\mathbf{e}^i \in \mathcal{A}^T$ . At the start of each trial  $t \in [T]$ , the learner views the sequence  $\langle \mathbf{e}_t^i \mid i \in [E] \rangle$ .

We can also view the experts alternatively as *confidence-rated predictors* over the set  $[K]$ : For each  $i \in [E]$  and  $t \in [T]$ , the vector  $\mathbf{e}_t^i$  can be viewed as suggesting the probability distribution  $\mathbf{e}_t^i / \|\mathbf{e}_t^i\|_1$  over  $[K]$ , but with confidence  $\|\mathbf{e}_t^i\|_1$ . We denote this confidence by  $c_{t,i} := \|\mathbf{e}_t^i\|_1$  and write  $\mathbf{c}_t := (c_{t,1}, \dots, c_{t,E})$ .

In this work we will refer to the *unnormalized relative entropy* defined by:

$$\Delta(\mathbf{u}, \mathbf{v}) := \sum_{i \in [E]} u_i \ln \left( \frac{u_i}{v_i} \right) - \|\mathbf{u}\|_1 + \|\mathbf{v}\|_1,$$

for any  $\mathbf{u}, \mathbf{v} \in \mathbb{R}_+^E$ . We will also use the Iverson bracket notation  $\llbracket \text{PRED} \rrbracket$  as the indicator function, meaning that it is equal to 1 if PRED is true, and 0 otherwise.

### 3. Main Result

Our main result is represented by the bound on the cumulative reward of our algorithm CBA. We note that any *weight* vector  $\mathbf{u} \in \mathbb{R}_+^E$  induces a matrix  $\boldsymbol{\pi}(\mathbf{u}) \in \mathbb{R}_+^{T \times K}$  defined by

$$\boldsymbol{\pi}(\mathbf{u}) := \sum_{i \in [E]} u_i \mathbf{e}^i,$$

which is the linear combination of the experts with coefficients given by  $\mathbf{u}$ . However, only some such linear combinations generate valid policies. Thus, we define

$$\mathcal{V} := \{\mathbf{u} \in \mathbb{R}_+^E, \mid \boldsymbol{\pi}(\mathbf{u}) \in \mathcal{A}^T\}$$

as the set of all weight vectors that generate valid policies. Particularly, note that  $\mathbf{u} \in \mathcal{V}$  if and only if, on every trial  $t$ , the weighted sum of the confidences  $\mathbf{u} \cdot \mathbf{c}_t$  is no greater than one. Given some  $\mathbf{u} \in \mathcal{V}$  we define

$$\rho(\mathbf{u}) := \sum_{t \in [T]} \mathbf{r}_t \cdot \boldsymbol{\pi}_t(\mathbf{u}),$$

which would be the expected cumulative reward of the learner if it was to follow the policy  $\boldsymbol{\pi}(\mathbf{u})$ . We point out that the learner does not know  $\mathcal{V}$  or the function  $\boldsymbol{\pi}$  a-priori.

The following theorem (proved in Section 5) allows us to bound the regret of CBA with respect to any valid linear combination  $\mathbf{u}$  of experts.

**Theorem 3.1.** *CBA takes parameters  $\eta \in (0, 1)$  and  $\mathbf{w}_1 \in \mathbb{R}_+^E$ . For any  $\mathbf{u} \in \mathcal{V}$  the expected cumulative reward of CBA is bounded below by:*

$$\sum_{t \in [T]} \mathbb{E}[r_{t,a_t}] \geq \mathbb{E}[\rho(\mathbf{u})] - \frac{\Delta(\mathbf{u}, \mathbf{w}_1)}{\eta} - \eta(12K + 2)T$$

where the expectations are with respect to the randomization of CBA's strategy. The per-trial time runtime complexity of CBA is in  $\mathcal{O}(KE)$ .

We now compare our bound to that of previous algorithms. Firstly, EXP4 can only achieve bounds relative to a  $\mathbf{u} \in \mathcal{V}$  with  $\|\mathbf{u}\|_1 = 1$ , in which case it essentially matches our bound but with  $12K + 2$  replaced by  $8K + 8$ . Hence, for any  $\mathbf{u} \in \mathcal{V}$  the EXP4 bound essentially replaces the term  $\rho(\mathbf{u})$  in our bound by  $\rho(\mathbf{u})/\|\mathbf{u}\|_1$ . Note that  $\|\mathbf{u}\|_1$  could be as high as the number of experts which implies we can dramatically outperform EXP4. When viewing our experts as confidence-rated predictors, we note that previous algorithms for this setting only give bounds on a weighted sum of the per-trial rewards where the weight on each trial is  $\mathbf{u} \cdot \mathbf{c}_t$  for some

---

#### Algorithm 1 CBA( $\mathbf{w}_1, \eta$ )

---

**For**  $t = 1, 2, \dots, T$  **do**:

1. For all  $i \in [E]$  receive  $\mathbf{e}_t^i$
2. For all  $i \in [E]$  set  $c_{t,i} \leftarrow \|\mathbf{e}_t^i\|_1$
3. **If**  $\|\mathbf{c}_t\|_1 \leq 1$  **then**:

(a) Set  $\tilde{\mathbf{w}}_t \leftarrow \mathbf{w}_t$

4. **Else**:

(a) By interval bisection find  $\lambda > 0$  such that:

$$\sum_{i \in [E]} c_{t,i} w_{t,i} \exp(-\lambda c_{t,i}) = 1$$

(b) For all  $i \in [E]$  set  $\tilde{w}_{t,i} \leftarrow w_{t,i} \exp(-\lambda c_{t,i})$

5. **Set**:

$$\mathbf{s}_t \leftarrow \sum_{i \in [E]} \tilde{w}_{t,i} \mathbf{e}_t^i$$

6. Draw  $a_t \sim \mathbf{s}_t$

7. Receive  $r_{t,a_t}$

8. For all  $a \in [K]$  set:

$$\hat{r}_{t,a} \leftarrow 1 - \llbracket a = a_t \rrbracket (1 - r_{t,a_t}) / s_{t,a_t}$$

9. For all  $i \in [E]$  set  $w_{(t+1),i} \leftarrow \tilde{w}_{t,i} \exp(\eta \mathbf{e}_t^i \cdot \hat{\mathbf{r}}_t)$

---

$\mathbf{u} \in \mathcal{V}$ . This is only a cumulative reward bound when  $\mathbf{u} \cdot \mathbf{c}_t = 1$  for all  $t \in [T]$ , and finding such a  $\mathbf{u}$  is typically impossible. When there does exist a  $\mathbf{u}$  that satisfies this constraint, the reward relative to  $\mathbf{u}$  is essentially the same as for us (Blum & Mansour, 2007). However, there will often be another value of  $\mathbf{u}$  that will give us a much better bound, as we shall show in Section 6.

### 4. The CBA Algorithm

The CBA algorithm is given in Algorithm 1. In this section, we describe its derivation via a modification of the classic *mirror descent* algorithm.

Our modification of mirror descent is based on the following mathematical objects. For all  $t \in [T]$  we first define:

$$\mathcal{V}_t := \{\mathbf{v} \in \mathbb{R}_+^E \mid \|\boldsymbol{\pi}_t(\mathbf{v})\|_1 \leq 1\}$$

which is the set of all weight vectors that give rise to linear combinations producing valid stochastic actions at trial  $t$ . Given some  $t \in [T]$ , we define our *objective function*  $\rho_t : \mathcal{V}_t \rightarrow [-1, 1]$  as

$$\rho_t(\mathbf{v}) := \mathbf{r}_t \cdot \boldsymbol{\pi}_t(\mathbf{v}) \text{ for all } \mathbf{v} \in \mathcal{V}_t.$$

Like mirror descent, CBA maintains, on each trial  $t \in [T]$ , a weight vector  $\mathbf{w}_t \in \mathbb{R}_+^E$ . However, unlike mirror descent on the simplex, we do not keep  $\mathbf{w}_t$  normalized, but we will

instead project it into  $\mathcal{V}_t$  at the start of trial  $t$ , producing a vector  $\tilde{\mathbf{w}}_t$ . Also, unlike mirror descent, CBA does not use the actual gradient (which it does not know) of  $\rho_t$  at  $\tilde{\mathbf{w}}_t$ , but uses an unbiased estimator. Specifically, on each trial  $t \in [T]$ , CBA does the following:

1. Set  $\tilde{\mathbf{w}}_t \leftarrow \operatorname{argmin}_{\mathbf{v} \in \mathcal{V}_t} \Delta(\mathbf{v}, \mathbf{w}_t)$
2. Randomly construct a vector  $\mathbf{g}_t \in \mathbb{R}^E$  such that  $\mathbb{E}[\mathbf{g}_t] = \nabla \rho_t(\tilde{\mathbf{w}}_t)$
3. Set  $\mathbf{w}_{t+1} \leftarrow \operatorname{argmin}_{\mathbf{v} \in \mathbb{R}_+^E} (\eta \mathbf{g}_t \cdot (\tilde{\mathbf{w}}_t - \mathbf{v}) + \Delta(\mathbf{v}, \tilde{\mathbf{w}}_t))$

This naturally raises two questions: how is  $a_t$  selected and how is  $\mathbf{g}_t$  constructed? On each trial  $t \in [T]$  we define

$$\mathbf{s}_t := \sum_{i \in [E]} \tilde{w}_{t,i} \mathbf{e}_t^i,$$

which is the stochastic action generated by the linear combination  $\tilde{\mathbf{w}}_t$ , and select  $a_t \sim \mathbf{s}_t$ . Note that:

$$\mathbb{E}[r_{t,a_t}] = \rho_t(\tilde{\mathbf{w}}_t) \quad (1)$$

which confirms that  $\rho_t$  is indeed our objective function at trial  $t$ . Once  $r_{t,a_t}$  is revealed to us we can go ahead and construct the gradient estimator  $\mathbf{g}_t$ . It is important for our analysis that we construct this estimator in a specific way. Inspired by EXP4 we first define a reward estimator  $\hat{r}_t$  such that for all  $a \in [K]$  we have:

$$\hat{r}_{t,a} := 1 - \mathbb{I}[a = a_t](1 - r_{t,a_t})/s_{t,a}.$$

This reward estimate is unbiased as:

$$\mathbb{E}[\hat{r}_{t,a}] = 1 - \Pr[a = a_t](1 - r_{t,a_t})/s_{t,a} = r_{t,a}.$$

We then define, for all  $i \in [E]$ , the component:

$$g_{t,i} := \mathbf{e}_t^i \cdot \hat{\mathbf{r}}_t.$$

Note that for all  $i \in [E]$  we have:

$$\mathbb{E}[g_{t,i}] = \mathbf{e}_t^i \cdot \mathbb{E}[\hat{\mathbf{r}}_t] = \mathbf{e}_t^i \cdot \mathbf{r}_t = \partial_i \rho_t(\tilde{\mathbf{w}}_t)$$

so that  $\mathbb{E}[\mathbf{g}_t] = \nabla \rho_t(\tilde{\mathbf{w}}_t)$  as required.

Now that we defined the process by which CBA operates we must show how to compute  $\tilde{\mathbf{w}}_t$  and  $\mathbf{w}_{t+1}$ . First we show how to compute  $\tilde{\mathbf{w}}_t$  from  $\mathbf{w}_t$ . If  $\|\mathbf{c}_t\|_1 \leq 1$  it holds that  $\mathbf{w}_t \in \mathcal{V}_t$  so we immediately have  $\tilde{\mathbf{w}}_t = \mathbf{w}_t$ . Otherwise we must find  $\tilde{\mathbf{w}}_t \in \mathbb{R}_+^E$  that minimizes  $\Delta(\tilde{\mathbf{w}}_t, \mathbf{w}_t)$  subject to the constraint:

$$\sum_{i \in [E]} \tilde{w}_{t,i} c_{t,i} = 1,$$

which is equivalent to the constraint that  $\|\pi(\tilde{\mathbf{w}}_t)\|_1 = 1$ . Hence, by Lagrange's theorem there exists  $\lambda$  such that:

$$\nabla_{\tilde{\mathbf{w}}_t} \left( \Delta(\tilde{\mathbf{w}}_t, \mathbf{w}_t) + \lambda \sum_{i \in [E]} \tilde{w}_{t,i} c_{t,i} \right) = 0$$

which is solved by setting, for all  $i \in [E]$ :

$$\tilde{w}_{t,i} := w_{t,i} \exp(-\lambda c_{t,i}).$$

The constraint is then satisfied if  $\lambda$  is such that:

$$\sum_{i \in [E]} c_{t,i} w_{t,i} \exp(-\lambda c_{t,i}) = 1.$$

Since this function is monotonic decreasing,  $\lambda$  can be found by interval bisection.

Turning to the computation of  $\mathbf{w}_{t+1}$ , since it is unconstrained it is found by the equation:

$$\nabla_{\mathbf{w}_{t+1}} (\mathbf{g}_t \cdot \mathbf{w}_{t+1} + \eta^{-1} \Delta(\mathbf{w}_{t+1}, \tilde{\mathbf{w}}_t)) = 0.$$

which is solved by setting, for all  $i \in [E]$ :

$$w_{(t+1),i} := \tilde{w}_{t,i} \exp(\eta g_{t,i}). \quad (2)$$

## 5. CBA Analysis

Here we prove Theorem 3.1 from the modification of mirror descent (and the specific construction of  $\mathbf{g}_t$ ) given in Section 4. Whenever we take expectations in this analysis they are over the draw of  $a_t$  from  $\mathbf{s}_t$  for some  $t \in [T]$ . As for mirror descent, our analysis hinges on the following classic lemma:

**Lemma 5.1.** *Given any convex set  $\mathcal{C} \subseteq \mathbb{R}_+^E$ , any convex function  $\xi : \mathbb{R}_+^E \rightarrow \mathbb{R}$ , any  $\mathbf{q} \in \mathcal{C}$  and any  $\mathbf{z} \in \mathbb{R}_+^E$  with:*

$$\mathbf{q} = \operatorname{argmin}_{\mathbf{v} \in \mathcal{C}} (\xi(\mathbf{v}) + \Delta(\mathbf{v}, \mathbf{z})),$$

then for all  $\mathbf{u} \in \mathcal{C}$  we have:

$$\xi(\mathbf{u}) + \Delta(\mathbf{u}, \mathbf{z}) \geq \xi(\mathbf{q}) + \Delta(\mathbf{u}, \mathbf{q}).$$

*Proof.* Theorem 9.12 in Beck (2017) shows that the theorem holds if  $\Delta$  is Bregman divergence. In our case  $\Delta$  is indeed a Bregman divergence: that of the convex function  $f : \mathbb{R}_+^E \rightarrow \mathbb{R}$  for all  $\mathbf{v} \in \mathbb{R}_+^E$  defined by:

$$f(\mathbf{v}) := \sum_{i \in [E]} v_i \ln(v_i),$$

which concludes the proof.  $\square$

Choose any  $\mathbf{u} \in \mathcal{V}$  and  $t \in [T]$ . We immediately have  $\mathcal{V} \subseteq \mathcal{V}_t$  by definition, and therefore  $\mathbf{u} \in \mathcal{V}_t$ . Hence, by setting  $\xi$  such that  $\xi(\mathbf{v}) := 0$  for all  $\mathbf{v} \in \mathbb{R}_+^E$ , setting  $\mathcal{C} \in \mathcal{V}_t$  and setting  $\mathbf{z} = \mathbf{w}_t$  in Lemma 5.1 we have  $\mathbf{q} = \tilde{\mathbf{w}}_t$  so that:

$$\Delta(\mathbf{u}, \mathbf{w}_t) \geq \Delta(\mathbf{u}, \tilde{\mathbf{w}}_t). \quad (3)$$

Alternatively, by setting  $\xi$  such that  $\xi(\mathbf{v}) := \eta \mathbf{g}_t \cdot (\tilde{\mathbf{w}}_t - \mathbf{v})$  for all  $\mathbf{v} \in \mathbb{R}_+^E$ , setting  $\mathcal{C} = \mathbb{R}_+^E$  and setting  $\mathbf{z} = \tilde{\mathbf{w}}_t$  in Lemma 5.1 we have  $\mathbf{q} = \mathbf{w}_{t+1}$  so that:

$$\begin{aligned} & \eta \mathbf{g}_t \cdot (\tilde{\mathbf{w}}_t - \mathbf{u}) + \Delta(\mathbf{u}, \tilde{\mathbf{w}}_t) \\ & \geq \eta \mathbf{g}_t \cdot (\tilde{\mathbf{w}}_t - \mathbf{w}_{t+1}) + \Delta(\mathbf{u}, \mathbf{w}_{t+1}). \end{aligned} \quad (4)$$

Since  $\mathbb{E}[g_t] = \nabla \rho_t(\tilde{\mathbf{w}}_t)$  and  $\rho_t$  is linear we have:

$$\mathbb{E}[g_t \cdot (\tilde{\mathbf{w}}_t - \mathbf{u})] = \rho_t(\tilde{\mathbf{w}}_t) - \rho_t(\mathbf{u}). \quad (5)$$

In what follows we use the fact that for all  $x \leq 1$  we have:

$$x(1 - \exp(x)) \geq -2x^2. \quad (6)$$

For all  $i \in [E]$ , we have, by definition, that  $g_{t,i} = e_t^i \cdot \hat{\mathbf{r}}_t$  so by Equation (2) we have:

$$g_t \cdot (\tilde{\mathbf{w}}_t - \mathbf{w}_{t+1}) = \sum_{i \in [E]} \tilde{w}_{t,i} e_t^i \cdot \hat{\mathbf{r}}_t (1 - \exp(\eta e_t^i \cdot \hat{\mathbf{r}}_t)).$$

Since, for all  $a \in [K]$ , we have  $\hat{r}_{t,a} \leq 1$  and hence, as  $\eta < 1$  and, for all  $i \in [E]$  we have  $\|e_t^i\|_1 \leq 1$ , we can invoke Equation (6), which gives us:

$$\eta g_t \cdot (\tilde{\mathbf{w}}_t - \mathbf{w}_{t+1}) \geq -2 \sum_{i \in [E]} \tilde{w}_{t,i} (\eta e_t^i \cdot \hat{\mathbf{r}}_t)^2. \quad (7)$$

By definition of  $\hat{\mathbf{r}}_t$  we have, for all  $i \in [E]$ , that:

$$e_t^i \cdot \hat{\mathbf{r}}_t = \|e_t^i\|_1 + e_{t,a_t}^i (1 - r_{t,a_t}) / s_{t,a_t} \leq c_{t,i} + 2e_{t,a_t}^i / s_{t,a_t}$$

so that since, for all  $a \in [K]$ , we have  $\Pr[a_t = a] = s_{t,a}$  we also have:

$$\mathbb{E}[(e_t^i \cdot \hat{\mathbf{r}}_t)^2] \leq c_{t,i}^2 + \sum_{a \in [K]} (2e_{t,a}^i c_{t,i} + 4(e_{t,a}^i)^2 / s_{t,a}). \quad (8)$$

Since, for all  $i \in [E]$  and  $a \in [K]$ , we have  $e_{t,a}^i \leq 1$  and  $c_{t,i} \leq 1$  and hence also  $c_{t,i}^2 \leq c_{t,i}$  we then have:

$$\mathbb{E}[(e_t^i \cdot \hat{\mathbf{r}}_t)^2] \leq (2K + 1)c_{t,i} + 4 \sum_{a \in [K]} e_{t,a}^i / s_{t,a}. \quad (9)$$

Note that since  $\tilde{\mathbf{w}}_t \in \mathcal{V}_t$  we have:

$$\sum_{i \in [E]} \tilde{w}_{t,i} c_{t,i} \leq 1. \quad (10)$$

Also, by definition of  $s_t$  we have:

$$\begin{aligned} \sum_{i \in [E]} \tilde{w}_{t,i} \sum_{a \in [K]} e_{t,a}^i / s_{t,a} &= \sum_{a \in [K]} \frac{1}{s_{t,a}} \sum_{i \in [E]} \tilde{w}_{t,i} e_{t,a}^i \\ &= \sum_{a \in [K]} \frac{1}{s_{t,a}} s_{t,a} = K. \end{aligned} \quad (11)$$

Multiplying Inequality (9) by  $\tilde{w}_{t,i}$ , summing over all  $i \in [E]$ , and then substituting in Inequality (10) and Equation (11) gives us:

$$\sum_{i \in [E]} \tilde{w}_{t,i} \mathbb{E}[(e_t^i \cdot \hat{\mathbf{r}}_t)^2] \leq (2K + 1) + 4K = 6K + 1. \quad (12)$$

---

**Algorithm 2** QUERY( $q$ )
 

---

1. For all  $i \in [n] \cup \{0\}$  let  $\gamma_i$  be the ancestor of  $q$  at depth  $i$  in  $\mathcal{D}$
  2. Set  $\sigma_n \leftarrow \psi(\gamma_n)\phi(\gamma_n)$
  3. Climb  $\mathcal{D}$  from  $\gamma_{n-1}$  to  $\gamma_0$ . When at  $\gamma_i$  do as follows:
    - (a) If  $\gamma_{i+1} = \triangleleft(\gamma_i)$  then set  $\sigma_i \leftarrow \phi(\gamma_i)(\sigma_{i+1} + \psi(\triangleright(\gamma_i))\phi(\triangleright(\gamma_i)))$
    - (b) If  $\gamma_{i+1} = \triangleright(\gamma_i)$  then set  $\sigma_i \leftarrow \phi(\gamma_i)\sigma_{i+1}$
  4. Return  $\sigma_0$
- 

Taking expectations on Inequality (7) and substituting in Inequality (12) (after taking expectations) gives us:

$$\mathbb{E}[\eta g_t \cdot (\tilde{\mathbf{w}}_t - \mathbf{w}_{t+1})] \geq -\eta^2(12K + 2). \quad (13)$$

Taking expectations (over the draw  $a_t \sim s_t$ ) on Inequality (4), substituting in Inequalities (3), (5) and (13), and then rearranging gives us:

$$\begin{aligned} \Delta(\mathbf{u}, \mathbf{w}_t) - \mathbb{E}[\Delta(\mathbf{u}, \mathbf{w}_{t+1})] \\ \geq \eta(\rho_t(\mathbf{u}) - \rho_t(\tilde{\mathbf{w}}_t)) - \eta^2(12K + 2). \end{aligned}$$

Summing this inequality over all  $t \in [T]$ , taking expectations (over the entire sequence of action draws) and noting that  $\Delta(\mathbf{u}, \mathbf{w}_{T+1}) > 0$  gives us:

$$\Delta(\mathbf{u}, \mathbf{w}_1) \geq \eta \sum_{t \in [T]} \mathbb{E}[\rho_t(\mathbf{u}) - \rho_t(\tilde{\mathbf{w}}_t)] - \eta^2(12K + 2)T.$$

Substituting in Equation (1) and rearranging then gives us, by definition of  $\rho$  and  $\rho_t$ , the required goal:

$$\sum_{t \in [T]} \mathbb{E}[r_{t,a_t}] \geq \mathbb{E}[\rho(\mathbf{u})] - \Delta(\mathbf{u}, \mathbf{w}_1) / \eta - \eta(12K + 2)T. \quad \blacksquare$$

## 6. Efficient Learning with Metric Balls

We now give a simple example: that of finding disjoint balls in a finite space endowed with a distance function. We will also give subroutines that speed up CBA in this problem. Specifically, we have a set of *contexts*  $\mathcal{X}$  with  $|\mathcal{X}| = N$  for some  $N \in \mathbb{N}$ , as well as a *distance* function  $d : \mathcal{X} \times \mathcal{X} \rightarrow \mathbb{R}_+$  known to the learner a-priori. A-priori nature selects a sequence:  $\langle (x_t, \mathbf{r}_t) \in \mathcal{X} \times [-1, 1]^K \mid t \in [T] \rangle$ , but does not reveal it to the learner. For all  $t \in [T]$  we define  $r_{t,\square} := 0$ . On each trial  $t \in [T]$  the following happens:

1. The context  $x_t$  is revealed to the learner.
2. the learner selects an action  $a_t \in [K] \cup \{\square\}$ .
3. the learner sees and incurs reward  $r_{t,a_t} \in [-1, 1]$ .

Our cumulative reward bound will be based on the notion of a *ball*. Specifically, a ball is any set  $\mathcal{B} \subseteq \mathcal{X}$  in which there

**Algorithm 3** UPDATE( $q, p$ )

1. For all  $i \in [n] \cup \{0\}$  let  $\gamma_i$  be the ancestor of  $q$  at depth  $i$  in  $\mathcal{D}$
2. Descend  $\mathcal{D}$  from  $\gamma_0$  to  $\gamma_{n-1}$ . When at  $\gamma_i$  set:
  - (a)  $\phi(\triangleleft(\gamma_i)) \leftarrow \phi(\gamma_i)\phi(\triangleleft(\gamma_i))$
  - (b)  $\phi(\triangleright(\gamma_i)) \leftarrow \phi(\gamma_i)\phi(\triangleright(\gamma_i))$
  - (c)  $\phi(\gamma_i) \leftarrow 1$
3. For all  $i \in [n-1] \cup \{0\}$ , if  $\gamma_{i+1} = \triangleleft(\gamma_i)$  then set  $\phi(\triangleright(\gamma_i)) \leftarrow p\phi(\triangleright(\gamma_i))$
4. Set  $\phi(\gamma_n) \leftarrow p\phi(\gamma_n)$
5. Climb  $\mathcal{D}$  from  $\gamma_{n-1}$  to  $\gamma_0$ . When at  $\gamma_i$  set:
 
$$\psi(\gamma_i) \leftarrow \psi(\triangleleft(\gamma_i))\phi(\triangleleft(\gamma_i)) + \psi(\triangleright(\gamma_i))\phi(\triangleright(\gamma_i))$$

exists some  $x \in \mathcal{X}$  and  $\delta \in \mathbb{R}_+$  with:

$$\mathcal{B} = \{z \in \mathcal{X} \mid d(x, z) \leq \delta\}.$$

We now give the reward and time complexity bounds for the implementation of CBA that will follow:

**Theorem 6.1.** *Given any  $M \in \mathbb{N}$  we can implement CBA such that for any sequence of disjoint balls  $\langle \mathcal{B}_j \mid j \in [M] \rangle$  with corresponding actions  $\langle b_j \in [K] \mid j \in [M] \rangle$  we have:*

$$\begin{aligned} \sum_{t \in [T]} \mathbb{E}[r_{t,a_t}] &\geq \sum_{t \in [T]} \sum_{j \in [M]} \mathbb{1}[x_t \in \mathcal{B}_j] r_{t,b_j} \\ &\quad - \sqrt{4M \ln(N)(6K+1)T}. \end{aligned}$$

The per-trial time complexity of this implementation of CBA is in  $\mathcal{O}(KN \ln(N))$ .

We briefly comment on the term:  $\sum_{j \in [M]} \mathbb{1}[x_t \in \mathcal{B}_j] r_{t,b_j}$ , that appears in the theorem statement. If  $x_t$  does not belong to any of the balls in  $\langle \mathcal{B}_j \mid j \in [M] \rangle$  then this term is equal to zero (which is the reward of abstaining). Otherwise, since the balls are disjoint,  $x_t$  belongs to exactly one of them and the term is equal to the reward induced by the action that corresponds to that ball. In other words, the total cumulative reward is bounded relative to that of the policy that abstains whenever  $x_t$  is outside the union of the balls and otherwise selects the action corresponding to the ball that  $x_t$  lies in.

Note that the vast improvement in our reward bound is over that of SPECIALISTEXP with abstention as one of the actions. In order to get a reward bound for SPECIALISTEXP, the sets in which the specialists are awake must partition the set  $\mathcal{X}$ . This means that we must add to our  $M$  balls a disjoint covering (by balls) of the complement of the union of the original  $M$  balls. Remark that the added balls correspond to the sets in which the specialists predicting the abstention action are awake. Typically this would require a huge number of balls so that the total number of specialists is huge (much larger than  $M$ ); this huge number of specialists essentially replacing the term  $M$  in our reward

bound. Furthermore, in Appendix A, we show that the same implementation of CBA is capable of learning a weighted set of overlapping balls, as long as the sum of the weights of the balls covering any context is bounded above by one, which SPECIALISTEXP cannot do in general.

The choice of experts for CBA that leads to Theorem 6.1 is defined by the set of ball-action pairs so that  $E = N^2K$  and for each ball  $\mathcal{B}$  and action  $a \in [K]$  there exists a unique  $i \in [E]$  such that for all  $t \in [T]$  and  $b \in [K]$  we have:  $e_{t,b}^i := \mathbb{1}[x_t \in \mathcal{B}][b = a]$ . By choosing  $w_{1,i} = M/N^2$  for all  $i \in [E]$ , and choosing  $\eta := (M \ln(N)/(6K+1)T)^{-1/2}$ . Theorem 3.1 implies the reward bound in Theorem 6.1.

The per-trial time complexity of a direct implementation of CBA for this set of experts would be  $\mathcal{O}(KN^2)$ . We now show how to implement CBA in a per-trial time of only  $\mathcal{O}(KN \ln(N))$ . To do this first note that we can assume, without loss of generality, that for all  $q, x, z \in \mathcal{X}$  with  $x \neq z$  we have  $d(q, x) \neq d(q, z)$  since ties can be broken arbitrarily and balls can be duplicated.

Given  $x, z \in \mathcal{X}$ ,  $a \in [K]$  and  $t \in [T]$  we let  $y_{t,a}(x, z) := w_{t,i}$  and  $\tilde{y}_{t,a}(x, z) := \tilde{w}_{t,i}$  where  $i$  is the index of the expert corresponding to the ball-action pair with ball:  $\{q \in \mathcal{X} \mid d(q, x) \leq d(x, z)\}$ , and action  $a$ . Given  $x, z \in \mathcal{X}$  let  $\mathcal{E}(x, z) := \{q \in \mathcal{X} \mid d(q, x) \geq d(x, z)\}$ . It is straightforward to derive the following equations for the quantities in CBA at trial  $t \in [T]$ . First we have:

$$\|\mathbf{c}_t\|_1 = \sum_{a \in [K]} \sum_{x \in \mathcal{X}} \sum_{z \in \mathcal{E}(x, x_t)} y_{t,a}(x, z).$$

For all  $x, z \in \mathcal{X}$  and  $a \in [K]$  we have the following:

- If  $\|\mathbf{c}_t\|_1 \leq 1$  or  $z \notin \mathcal{E}(x, x_t)$  then  $\tilde{y}_{t,a}(x, z) = y_{t,a}(x, z)$ .
- If  $\|\mathbf{c}_t\|_1 > 1$  and  $z \in \mathcal{E}(x, x_t)$  then  $\tilde{y}_{t,a}(x, z) = y_{t,a}(x, z) / \|\mathbf{c}_t\|_1$ .

For all  $a \in [K]$  we have:

$$s_{t,a} = \sum_{x \in \mathcal{X}} \sum_{z \in \mathcal{E}(x, x_t)} \tilde{y}_{t,a}(x, z).$$

Finally, for all  $x, z \in \mathcal{X}$  and  $a \in [K]$  we have the following:

$$y_{(t+1),a}(x, z) = \begin{cases} \tilde{y}_{t,a}(x, z) & \text{if } z \notin \mathcal{E}(x, x_t), \\ \tilde{y}_{t,a}(x, z) \exp(\eta e_t^i \cdot \hat{\mathbf{r}}_t) & \text{if } z \in \mathcal{E}(x, x_t). \end{cases}$$

Hence, to implement CBA we need, for each  $x \in \mathcal{X}$  and  $a \in [K]$ , a data structure that implicitly maintains a function  $h : \mathcal{X} \rightarrow \mathbb{R}^+$  and has the following two subroutines, that take parameters  $q \in \mathcal{X}$  and  $p \in \mathbb{R}_+$ .

1. QUERY( $q$ ): Compute  $\sum_{z \in \mathcal{E}(x, q)} h(z)$ .
2. UPDATE( $q, p$ ): Set  $h(z) \leftarrow ph(z)$  for all  $z \in \mathcal{E}(x, q)$ .

Now fix  $x \in \mathcal{X}$  and  $a \in [K]$ . Let  $h$  be as above. On each trial  $t \in [T]$  and for all  $z \in \mathcal{X}$ ,  $h(z)$  will start equal to  $y_{t,a}(x, z)$  and change to  $\tilde{y}_{t,a}(x, z)$  and then  $y_{(t+1),a}(x, z)$  by applying the UPDATE subroutine.

We now show how to implement these subroutines implicitly in a time of  $\mathcal{O}(\ln(N))$  as required. Without loss of generality, assume that  $N = 2^n$  for some  $n \in \mathbb{N}$ . Our data structure is based on a balanced binary tree  $\mathcal{D}$  whose leaves are the elements of  $\mathcal{X}$  in order of increasing distance from  $x$ . This implies that for any  $z \in \mathcal{X}$  we have that  $\mathcal{E}(x, z)$  is the set of leaves that do not lie on the left of  $z$ . Given a node  $v \in \mathcal{D}$  we let  $\uparrow(v)$  be the set of ancestors of  $v$  and let  $\Downarrow(v)$  be the set of all  $z \in \mathcal{X}$  which are descendants of  $v$ . For any internal node  $v$  let  $\triangleleft(v)$  and  $\triangleright(v)$  be the left and right children of  $v$  respectively.

We maintain functions  $\phi, \psi : \mathcal{D} \rightarrow \mathbb{R}_+$  such that for all  $v \in \mathcal{D}$  we have:

$$\psi(v) \prod_{v' \in \uparrow(v)} \phi(v') = \sum_{z \in \Downarrow(v)} h(z). \quad (14)$$

The pseudo-code for the subroutines QUERY and UPDATE are given in Algorithms 2 and 3 respectively. We now prove their correctness. We first consider the QUERY subroutine with parameter  $q \in \mathcal{X}$ . From Equation (14) we see that, by (reverse) induction on  $i \in [n] \cup \{0\}$ , we have:

$$\sigma_i \prod_{v' \in \uparrow(\gamma_i) \setminus \{\gamma_i\}} \phi(v') = \sum_{z \in \Downarrow(\gamma_i) \cap \mathcal{E}(x, q)} h(z).$$

Since  $\gamma_0$  is the root of  $\mathcal{D}$ , we have  $\sigma_0 = \sum_{z \in \mathcal{E}(x, q)} h(z)$  as required. Now consider the UPDATE subroutine with parameters  $q \in \mathcal{X}$  and  $p \in \mathbb{R}_+$ . Let  $h$  be the implicitly maintained function before the subroutine is called. For Equation (14) to hold after the subroutine is called we need:

$$\psi(v) \prod_{v' \in \uparrow(v)} \phi(v') = \sum_{z \in \Downarrow(v)} h'(z). \quad (15)$$

where for all  $z \in \mathcal{X}$  we have:

$$h'(z) := \llbracket z \notin \mathcal{E}(x, q) \rrbracket h(z) + \llbracket z \in \mathcal{E}(x, q) \rrbracket p h(z).$$

We shall now show that Equation (15) does indeed hold after the subroutine is called, which will complete the proof. To show this we consider each step of the subroutine in turn. After Step 2 we have (via induction) that:

- For all  $v \in \uparrow(q)$  we have  $\phi(v) = 1$ .
- For all  $v \in \mathcal{D} \setminus \uparrow(q)$  we have:

$$\psi(v) \prod_{v' \in \uparrow(v)} \phi(v') = \sum_{z \in \Downarrow(v)} h(z).$$

So, since  $\mathcal{E}(x, q)$  is the set of all  $z \in \mathcal{X}$  that do not lie to the left of  $q$  in  $\mathcal{D}$  we have that, after Step 4 of the algorithm, the following holds:

- For all  $v \in \uparrow(q)$  we have  $\phi(v) = 1$ ,
- For all  $v \in \mathcal{D} \setminus \uparrow(q)$  we have:

$$\psi(v) \prod_{v' \in \uparrow(v)} \phi(v') = \sum_{z \in \Downarrow(v)} h'(z).$$

Hence, by induction, we have that, after Step 5 of the algorithm, it is the case that for all  $v \in \uparrow(q)$  we have:  $\psi(v) = \sum_{z \in \Downarrow(v)} h'(z)$ . So since  $\phi(v) = 1$  for all  $v \in \uparrow(q)$  and Step 5 does not alter  $\phi(v)$  or  $\psi(v)$  for any  $v \in \mathcal{D} \setminus \uparrow(q)$  we have Equation (15). ■

## 7. Preliminary Experiments

We empirically evaluate our approach in the context of on-line multi-class node classification on a given graph with bandit feedback. At each time step, the algorithm is presented with a node chosen uniformly at random and must either predict an action from the set of possible actions  $[K]$  or abstain. The node can accept (resulting in a positive reward) or reject (resulting in a negative reward) the suggestion based on its preferred class with a certain probability. This can be seen as a special case of the metric space example from Section 6, where the context set  $\mathcal{X} = [N]$  corresponds to the node set. In general, we are not constrained to metric balls but can use arbitrary experts that correspond to set-action pairs of the form  $(\mathcal{B}, k) \in 2^{\mathcal{X}} \times [K]$ . We call any such set-action pair a *basis set*, and a set of basis sets a *basis*. For our experiments, we selected some representative bases used on learning tasks on graphs before, each leading to different inductive priors on the node labeling. For this reason, we will distinguish the different classes as *foreground classes* (classes in which the learning bias structure is supposed to hold) and *background classes* (nodes for which is better to abstain). We provide a short description of the basis sets here and refer to Appendix B for more details.

**Effective  $p$ -resistance basis  $d_p$ :** Balls given by the metric

$$d_p(i, j) := \left( \min_{\mathbf{u} \in \mathbb{R}^N} \sum_{u_i - u_j = 1} \sum_{s, t \in V} |u_s - u_t|^p \right)^{-1/p}.$$

We use  $d_1$ ,  $d_2$ , and  $d_\infty$  (Herbster & Lever, 2009).

**Louvain method basis (LVC):** Communities returned by the Louvain method (Blondel et al., 2008), processed by the greedy peeling algorithm (Lanciano et al., 2023).

**Geodesic intervals basis (INT):** All sets of the form  $I(x, y) := \{z \in \mathcal{X} \mid z \text{ is on a shortest } x\text{-}y \text{ path}\}$  for all  $x, y \in \mathcal{X}$  (Pelajo, 2013; Thiessen & Gärtner, 2021).

We compare our approach CBA using each of these bases on real-world and artificial graphs against the following baselines: an implementation of CONTEXTUALBANDIT from Slivkins (2011), the GABA-II algorithm proposed by Herbster et al. (2021), and an EXP3 instance for each data point. We use the following graphs for evaluation.

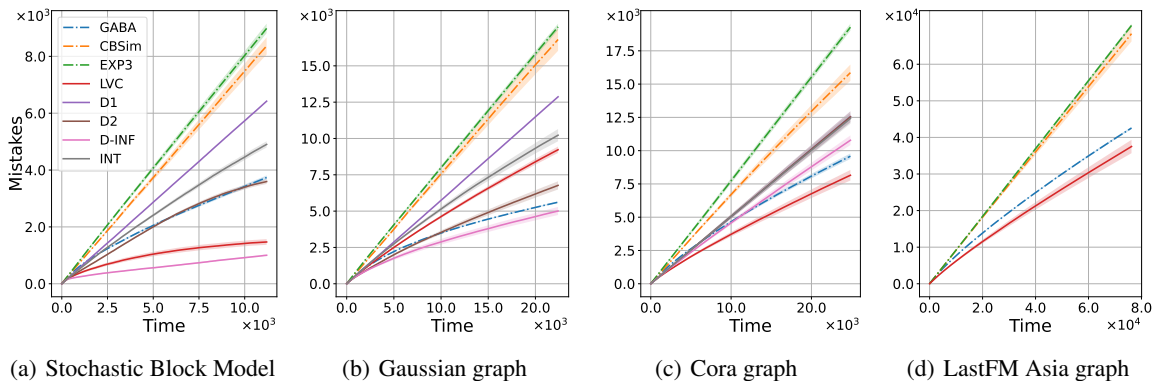


Figure 1. Results regarding the number of mistakes over time, the three main settings are presented from left to right: the Stochastic Block Model, Gaussian graph and LastFM Asia graph. In this context, D1, D2, and D-INF represent the  $p$ -norm bases, LVC represents the community detection basis, and INT represents the interval basis. The baselines, EXP3 for each context, Contextual Bandit with similarity, and GABA-II, are denoted as EXP3, CBSim, and GABA, respectively, and are represented with dashed lines. All the figures, display the data with 95% confidence intervals over 20 runs, calculated using the standard error multiplied by the  $z$ -score 1.96.

**Stochastic Block Model.** This graph, inspired by Holland et al. (1983), is generated by spawning an arbitrary number of disjoint cliques representing the foreground classes. Then an arbitrary number of background points are generated and connected to every possible point with a low probability. In Figure 1(a) are displayed the results for the case of  $F = 160$  nodes for each foreground class and  $B = 480$  nodes for the background class. Connecting each node of the background class with a probability of  $1/\sqrt{FB}$ .

**Gaussian graph.** The points on this graph are generated in a two-dimensional space using five different Gaussian distributions with zero mean. Four of them are positioned at the corners of the unit square, representing the foreground classes and having a relatively low standard deviation. Meanwhile, the fifth distribution, representing the background class, is centered within the square and is characterized by a larger standard deviation. The points are linked in a  $k$ -nearest neighbors graph. In Figure 1(b) are displayed the results for 160 nodes for each foreground class and a standard deviation of 0.2, 480 nodes for the background class with a standard deviation of 1.75, along with a 7-nearest neighbors graph.

**Real-world dataset.** We tested our approach on the Cora dataset (Sen et al., 2008) and the LastFM Asia dataset (Leskovec & Krevl, 2014). While both of these graphs contain both features and a graph, we exclusively utilized the largest connected component of each graph, resulting in 2485 nodes and 5069 edges for the Cora graph and 7624 nodes and 27806 edges for the LastFM Asia graph. Subsequently, we randomly chose a subset of three out of the original seven and eighteen classes, respectively, to serve as the background class. Additionally, we selected 15% of the nodes from the foreground classes randomly to represent

noise points, and we averaged the results over multiple runs, varying the labels chosen for noise. Both in Figures 1(c) and 1(d) we averaged over 5 different label sets as noise. For the LastFM Asia graph, we exclusively tested the LVC bases, as it is the most efficient one to compute given the large size of the graph.

**Results.** The results from both synthetically generated tests (Figures 1(a) and 1(b)) demonstrate the superiority of our method when compared to the baselines. In particular,  $d_\infty$ -balls delivered exceptional results for both graphs, implying that  $d_\infty$ -balls effectively cover the foreground classes as expected. For the Cora dataset (Figure 1(c)), we observed that our method outperforms GABA-II only when employing the community detection basis set. This similarity in performance is likely attributed to the dataset’s inherent lack of noise. Worth noting that the method we employed to inject noise into the dataset may not have been the optimal choice for this specific context. However, it is essential to highlight that our primary focus revolves around the abstention criteria, which plays a central role in ensuring the robustness of our model in the presence of noise. For the LastFM Asia dataset, our objective was to assess the practical feasibility of the model on a larger graph. We tested the LVC bases as they were the most promising and most efficient to compute. We outperform the baselines in our evaluation as shown in Figure 1(d) and further discussed in Appendix C.

In summary, our first results confirm what we expected: our approach excels when we choose basis functions that closely match the context’s structure. However, it also encounters difficulties when the chosen basis functions are not a good fit for the context. In Appendix C, the results for a wide range of different parameters used to generate the previously described graphs are displayed.



## Impact Statement

Given the theoretical nature of our work, we cannot foresee the shape of positive or negative societal impacts which this work may have in future.

## References

- Alamgir, M. and von Luxburg, U. Phase transition in the family of  $p$ -resistances. In *Proc. NIPS*, pp. 379–387, 2011.
- Auer, P. and Long, P. M. Structural results about on-line learning models with and without queries. *Mach. Learn.*, 36:147–181, 1999.
- Auer, P., Cesa-Bianchi, N., Freund, Y., and Schapire, R. E. The nonstochastic multiarmed bandit problem. *SIAM J. Comput.*, 32(1):48–77, 2002.
- Beck, A. *First-Order Methods in Optimization*. SIAM, 2017.
- Blondel, V. D., Guillaume, J.-L., Lambiotte, R., and Lefebvre, E. Fast unfolding of communities in large networks. *J. Stat. Mech. Theory Exp.*, 2008(10):P10008, 2008.
- Blum, A. and Mansour, Y. From external to internal regret. *J. Mach. Learn. Res.*, 8(6), 2007.
- Bressan, M., Cesa-Bianchi, N., Lattanzi, S., and Paudice, A. Exact recovery of clusters in finite metric spaces using oracle queries. In *Proc. COLT*, 2021.
- Chow, C. On optimum recognition error and reject tradeoff. *IEEE Trans. Inf. Theory*, 16(1):41–46, 1970.
- Chow, C.-K. An optimum character recognition system using decision functions. *IRE Trans. Electron. Comput.*, EC-6(4):247–254, 1957.
- Cortes, C., DeSalvo, G., Gentile, C., Mohri, M., and Yang, S. Online learning with abstention. In *Proc. ICML*, pp. 1059–1067, 2018.
- Cortes, C., DeSalvo, G., Gentile, C., Mohri, M., and Zhang, N. Online learning with dependent stochastic feedback graphs. In *Proc. ICML*, pp. 2154–2163, 2020.
- Doyle, P. G. and Snell, J. L. *Random Walks and Electric Networks*, volume 22 of *The Carus Mathematical Monographs*. American Mathematical Society, 1984.
- Floyd, R. W. Algorithm 97: shortest path. *Commun. ACM*, 5(6):345, 1962.
- Fortunato, S. Community detection in graphs. *Phys. Rep.*, 486(3):75–174, 2010.
- Freund, Y., Schapire, R. E., Singer, Y., and Warmuth, M. K. Using and combining predictors that specialize. In *Proc. STOC*, pp. 334–343, 1997.
- Gaillard, P., Stoltz, G., and Van Erven, T. A second-order bound with excess losses. In *Proc. COLT*, pp. 176–196, 2014.
- Gomory, R. E. and Hu, T. C. Multi-terminal network flows. *J. Soc. Ind. Appl. Math.*, 9(4):551–570, 1961.
- Hendrickx, K., Perini, L., Van der Plas, D., Meert, W., and Davis, J. Machine learning with a reject option: A survey. *arXiv preprint arXiv:2107.11277*, 2021.
- Herbster, M. and Lever, G. Predicting the labelling of a graph via minimum  $p$ -seminorm interpolation. In *Proc. COLT*, 2009.
- Herbster, M., Pasteris, S., Vitale, F., and Pontil, M. A gang of adversarial bandits. In *Proc. NeurIPS*, pp. 2265–2279, 2021.
- Holland, P. W., Laskey, K. B., and Leinhardt, S. Stochastic blockmodels: First steps. *Soc. Netw.*, 5(2):109–137, 1983.
- Lanciano, T., Miyauchi, A., Fazzone, A., and Bonchi, F. A survey on the densest subgraph problem and its variants. *arXiv*, arXiv:2303.14467, 2023.
- Lattimore, T. and Szepesvári, C. *Bandit Algorithms*. Cambridge University Press, 2020.
- Leskovec, J. and Krevl, A. SNAP Datasets: Stanford large network dataset collection. <http://snap.stanford.edu/data>, June 2014.
- Luo, H. and Schapire, R. E. Achieving all with no parameters: Adanormalhedge. In *Proc. COLT*, pp. 1286–1304, 2015.
- Neu, G. and Zhivotovskiy, N. Fast rates for online prediction with abstention. In *Proc. COLT*, pp. 3030–3048, 2020.
- Newman, M. E. and Girvan, M. Finding and evaluating community structure in networks. *Phys. Rev. E*, 69(2):026113, 2004.
- Pelayo, I. M. *Geodesic Convexity in Graphs*. Springer, 2013.
- Saito, S. and Herbster, M. Multi-class graph clustering via approximated effective  $p$ -resistance. In *Proc. ICML*, pp. 29697–29733, 2023.
- Schreuder, N. and Chzhen, E. Classification with abstention but without disparities. In *Proc. UAI*, pp. 1227–1236, 2021.

Sen, P., Namata, G., Bilgic, M., Getoor, L., Galligher, B., and Eliassi-Rad, T. Collective classification in network data. *AI Mag.*, 29(3):93–93, 2008.

Slivkins, A. Contextual bandits with similarity information. In *Proc. COLT*, pp. 679–702, 2011.

Thiessen, M. and Gärtner, T. Active learning of convex halfspaces on graphs. In *Proc. NeurIPS*, 2021.

Traag, V. A. Faster unfolding of communities: Speeding up the louvain algorithm. *Phys. Rev. E*, 92(3):032801, 2015.

van De Vel, M. L. *Theory of Convex Structures*. Elsevier, 1993.

## A. Overlapping balls extension

In this section, we present the theorem that allows us to present the results of overlapping balls as expressed in Section 6. Note that Theorem 6.1 is the special case of Theorem A.1 when the balls are disjoint and  $u_j = 1$  for all  $j \in [M]$ .

**Theorem A.1.** *Let  $M \in \mathbb{N}$  and  $\{(\mathcal{B}_j, b_j, u_j) \mid j \in [M]\}$  be any sequence such that  $\mathcal{B}_j$  is a ball,  $b_j \in [K]$  is an action, and  $u_j \in [0, 1]$  is such that for all  $x \in \mathcal{X}$  we have:*

$$\sum_{j \in [M]} \mathbb{1}[x \in \mathcal{B}_j] u_j \leq 1.$$

For all  $t \in [T]$  define:

$$r_t^* := \sum_{j \in [M]} \mathbb{1}[x_t \in \mathcal{B}_j] u_j r_{t, b_j},$$

which represents the reward of the policy induced by  $\{(\mathcal{B}_j, b_j, u_j) \mid j \in [M]\}$  on trial  $t$ . The regret of CBA, with the set of experts given in Section 6 and with correctly tuned parameters, is then bounded by:

$$\sum_{t \in [T]} r_t^* - \sum_{t \in [T]} \mathbb{E}[r_{t, a_t}] \in \mathcal{O} \left( \sqrt{\ln(KN)KT \sum_{j \in [M]} u_j} \right).$$

Its per-trial time complexity is:

$$\mathcal{O}(KN \ln(N)).$$

*Proof.* Direct from Theorem 3.1 using the experts (with efficient implementation) given in Section 6 □

## B. The Details of the Graph Bases

This section expands the definition and explanations for the bases we used in the Experiment. Remember that we refer to any set of experts that correspond to set-action pairs of the form  $(\mathcal{B}, k) \in 2^{\mathcal{X}} \times [K]$  as a *basis set*, and a set of basis sets as *basis*.

### B.1. $p$ -seminorm Balls on Graphs

As we see in Sec. 6, the CBA seems to work only for vector data. However, in the following sections, we explore how our CBA algorithm can be applied to graph data by creating a ball structure over the graph.

We first introduce the notations of a graph. A graph is a pair of *nodes*  $V := [N]$  and *edges*  $E$ . An edge connects two nodes, and we assume that our graph is *undirected* and *weighted*. For each edge  $\{i, j\} \in E$ , we denote its weight by  $c_{ij}$ . For convenience, for each pair of nodes  $i, j$  with  $\{i, j\} \notin E$ , we define  $c_{ij} = 0$ .

To form a ball over a graph, a family of metrics we are particularly interested in is given by  $p$ -norms on a given graph  $G$ . Let

$$d_p(i, j) := \left( \min_{\substack{\mathbf{u} \in \mathbb{R}^N \\ u_i - u_j = 1}} \sum_{s, t \in V} c_{st} |u_s - u_t|^p \right)^{-1/p}. \quad (16)$$

which is a well-defined metric for  $p \in [1, \infty)$  if the graph is connected and may be defined for  $p = \infty$  by taking the appropriate limits. When  $p = 2$  this is the square root of the *effective resistance* circuit between nodes  $i$  and  $j$  which comes from interpreting the graph as an electric circuit where the edges are unit resistors and the denominator of Equation (16) is the power required to maintain a unit voltage difference between  $u$  and  $v$  (Doyle & Snell, 1984). More generally,  $d_p(i, j)^p$  is known as  $p$ -(effective) resistance (Herbster & Lever, 2009; Alamgir & von Luxburg, 2011; Saito & Herbster, 2023). When  $p \in \{1, 2, \infty\}$  there are natural interpretation of the  $p$ -resistance. In the case of  $p = 1$ , we have that the effective is equal to one over the number of edge-disjoint paths between  $i$  and  $j$  which is equivalently one over the minimal cut that separates  $i$  from  $j$ . When  $p = 2$  it is the effective resistance as discussed above. And finally when  $p = \infty$  we have that  $d_\infty$  is the geodesic distance (shortest path) between  $i$  and  $j$ . Note that, interestingly, there are at most  $2N$  distinct balls for  $d_1$ ; as opposed to the general bound  $O(N^2)$  on the number of metric balls. This follows since  $d_1$  is an *ultrametric*. A nice feature of metric balls is that they are ordinal, i.e., we can take an increasing function of the distance and the distinct

are unchanged. The time complexity for each ball is as follows. For  $d_1$  ball, we compute every pair of distance in  $\mathcal{O}(N^3)$  using the Gomory-Hu tree (Gomory & Hu, 1961). For  $d_2$  ball, it is actually enough to compute the pseudoinverse of graph Laplacian once, which costs  $\mathcal{O}(N^3)$  (Doyle & Snell, 1984). For  $d_\infty$  ball, we can compute every pair of distance in  $\mathcal{O}(N^3)$  by Floyd–Warshall algorithm (Floyd, 1962).

## B.2. Community detection bases

In this section, we consider only bases formed via a set of subsets (a.k.a clusters)  $C \subseteq 2^{[N]}$ . Each of these subsets induces  $K$  basis elements: one for each action  $a \in [K]$ . Specifically, the basis element  $\beta : [N] \rightarrow [K \square]$  corresponding to the pair  $(C, a)$  is such that  $\beta(x)$  is equal to  $a$  whenever  $x \in C$  and equal to  $\square$  otherwise. Hence, in this section, we equate a basis with a set of subsets of  $[N]$ .

We can compute a basis for a given graph  $G = (V, E)$  using community detection algorithms. Community detection is one of the most well-studied operations for graphs, where the goal is to find a partition  $\{C_1, \dots, C_q\}$  of  $V$  (i.e.,  $\bigcup_{i=1}^q C_i = V$  and  $C_i \cap C_j = \emptyset$  for  $i \neq j$ ) so that each  $C_i$  is densely connected internally but sparsely connected to the rest of the graph (Fortunato, 2010). There are many community detection algorithms, all of which can be used here, but the most popular algorithm is the Louvain method (Blondel et al., 2008). We briefly describe how this algorithm works. The algorithm starts with an initial partition  $\{\{v\} \mid v \in V\}$  and aggregates the clusters iteratively: For each  $v \in V$ , compute the gain when moving  $v$  from its current cluster to its neighbors’ clusters and indeed move it to a cluster with the maximum gain (if the gain is positive). Note that the gain is evaluated using *modularity*, i.e., the most popular quality function for community detection (Newman & Girvan, 2004). The algorithm repeats this process until no movement is possible. Then the algorithm aggregates each cluster to a single super node (with appropriate addition of self-loops and change of edge weights) and repeats the above process on the coarse graph as long as the coarse graph is updated. Finally, the algorithm outputs the partition of  $V$  in which each cluster corresponds to each super node in the latest coarse graph. Note that it is widely recognized that the Louvain method works in  $\mathcal{O}(N \log N)$  in practice (Traag, 2015).

To obtain a finer-grained basis set, we apply the so-called greedy peeling algorithm for each  $C_i$  in the output of the Louvain method. For  $C_i \subseteq V$  and  $v \in C_i$ , we denote by  $d_{C_i}(v)$  the degree of  $v$  in the induced subgraph  $G[C_i]$ . For  $G[C_i]$ , the greedy peeling iteratively removes a node with the smallest degree in the currently remaining graph and obtains a sequence of node subsets from  $C_i$  to a singleton. Specifically, it works as follows: Set  $j \leftarrow |C_i|$  and  $C_i^{(j)} \leftarrow C_i$ . For each  $j = |C_i|, \dots, 2$ , compute  $v_{\min} \in \arg \min \{d_{C_i^{(j)}}(v) \mid v \in C_i^{(j)}\}$  and  $C_i^{(j-1)} \leftarrow C_i^{(j)} \setminus \{v_{\min}\}$ . Using a sophisticated data structure, this algorithm runs in linear time (Lanciano et al., 2023).

In summary, our community detection basis set is the collection of node subsets  $\{C_i^{(j)} \mid i = 1, \dots, q, j = 1, \dots, |C_i|\}$  together with  $\{\{v\} \mid v \in V\}$  for completeness.

## B.3. Graph convexity bases

An alternative to metric balls and communities are, for example, (geodesically) convex sets in a graph. They correspond to the inductive bias that if two nodes prefer the same action, then also the nodes on a shortest path between the two tend to prefer the same action. Geodesically convex sets are well-studied (van De Vel, 1993; Pelayo, 2013) and have been recently used in various learning settings on graphs (Bressan et al., 2021; Thiessen & Gärtner, 2021). Similarly to convex sets in the Euclidean space, a set  $C$  of nodes is *convex* if the nodes of any shortest path with endpoints in  $C$  are in  $C$ , as well. More formally, the (geodesic) *interval*  $I(u, v) = \{x \in V : x \text{ is on a shortest path between } u \text{ and } v\}$  of two nodes  $u$  and  $v$  contains all the nodes on a shortest path between them. For a set of node  $A$  we define  $I(A) = \bigcup_{a, b \in A} I(a, b)$  as a shorthand notation for the union of all pairwise intervals in  $A$ . A set  $A$  is (geodesically) convex iff  $I(A) = A$  and the *convex hull*  $\text{conv}(A)$  of a set  $A$  is the (unique) smallest convex set containing  $A$ . Note that for  $u, v \in V$ ,  $I(u, v)$  and  $\text{conv}(\{u, v\})$  are typically different sets. Indeed,  $I(u, v)$  is in general non-convex, as nodes on a shortest path between two nodes in  $I(u, v)$  (except for  $u, v$ ) are not necessarily contained in  $I(u, v)$ . As the total number of convex sets can be exponential in  $N$ , e.g., all subsets of a complete subgraph are convex, we consider the basis set consisting of all intervals:  $I(u, v)$  for  $u, v \in [N]$ . This involves  $\mathcal{O}(N^2)$  basis elements, each of size  $\mathcal{O}(N)$ . With a simple modification of the Floyd Warshall (Floyd, 1962) algorithm, computing the interval basis takes  $\mathcal{O}(N^3)$  time complexity.

### C. Additional Experimental Results

We thoroughly explored various configurations for the three graphs described in our experimental setup in Section 7. Figure 2 displays different settings for the number of nodes in each clique and noise levels.

As we compare the computational complexity of each basis set in Section B and the main results, the most intense computational load in the experiments will arise from the calculation of the basis set, which can be seen as an initialization step in our algorithm. The proposed methods have varying computational complexities, and an arbitrarily complex function can be employed to compute the basis set. Remark that, in the usual complexity comparison among online learning algorithms using experts, we compare the complexity *given* the experts. Practically, we use pre-computed bases or even human experts. Also note that due to the expensive complexity of the  $p$ -balls and the convex sets seen in Section B, we only conduct the LVC for LastFM Asia.

In Figure 3, we present multiple settings for generating the Gaussian graph. Here the title of each plot is “Foreground  $x,y$ ; Background  $x',y'$ ;  $k$ -NN,” which is explained as follows:  $x$  represents the number of nodes in each foreground class,  $x'$  represents the number of nodes in the background class,  $y$  represents the standard deviation of the Gaussians generating the foreground class,  $y'$  represents the standard deviation of the Gaussian generating the background class, and  $k$  represents the number of nearest neighbors used to generate the graph.

In Figure 4, we present the various labels chosen as noise for the Cora graph. In Figure 1(c), we presented the averages of all these different configurations. Here, we can see that the main behavior of the various bases is roughly maintained independently of the different labels chosen to be masked as background class.

In Figure 5, we present the various labels chosen as noise for the LastFM Asia graph. This graph comprises nodes representing LastFM users in Asian countries and edges representing mutual follower connections. Vertex features are extracted based on the artists liked by the users. During this initial analysis, we arbitrarily chose three out of eighteen possible labels to serve as the background class. In Figure 1(d), we presented the averages of all these different configurations. Varying the chosen background classes also produces different results, this is indeed due to the inherent lack of noise in the dataset. It is nice to see that regardless of the noise labels chosen, the behavior of our algorithm is always good, showing, as expected, that based on the amount of noise, we can just improve.

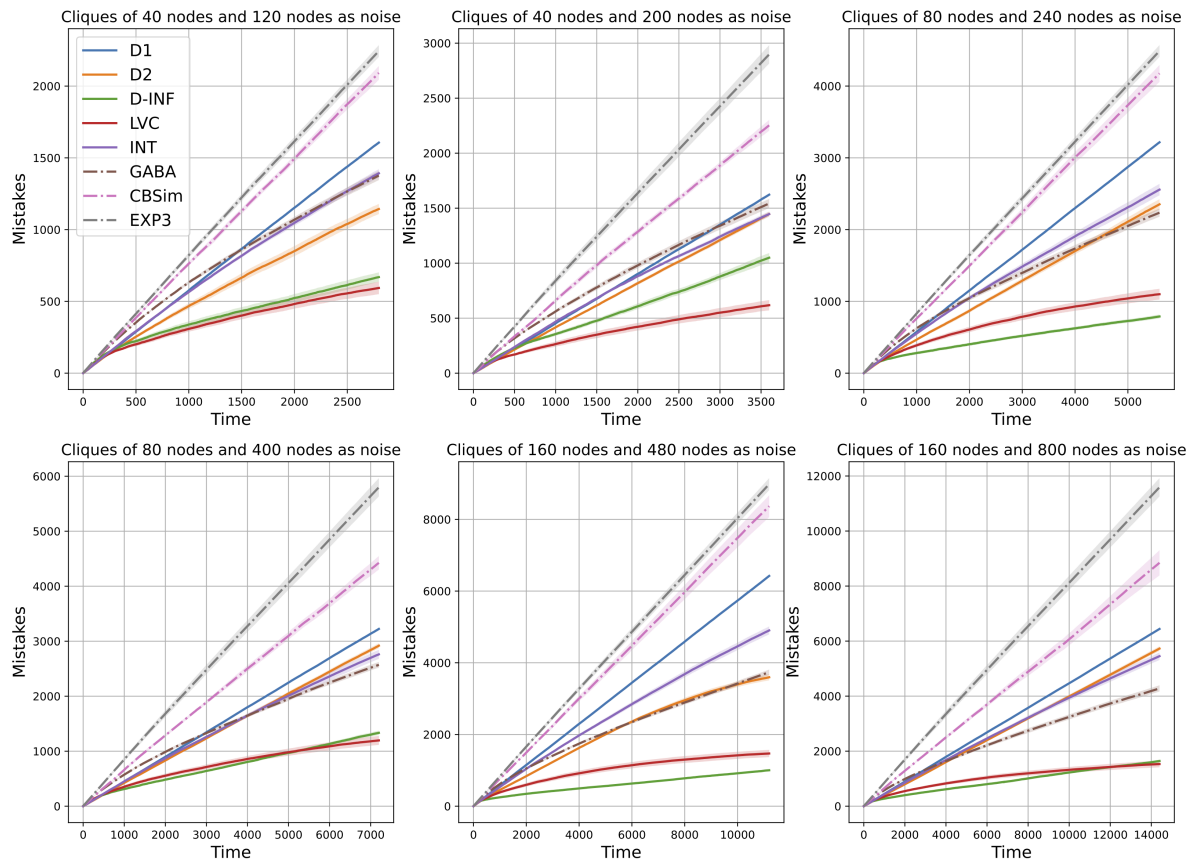


Figure 2. Stochastic Block Model results, dotted lines represent different baselines, while solid lines are used to represent various results.

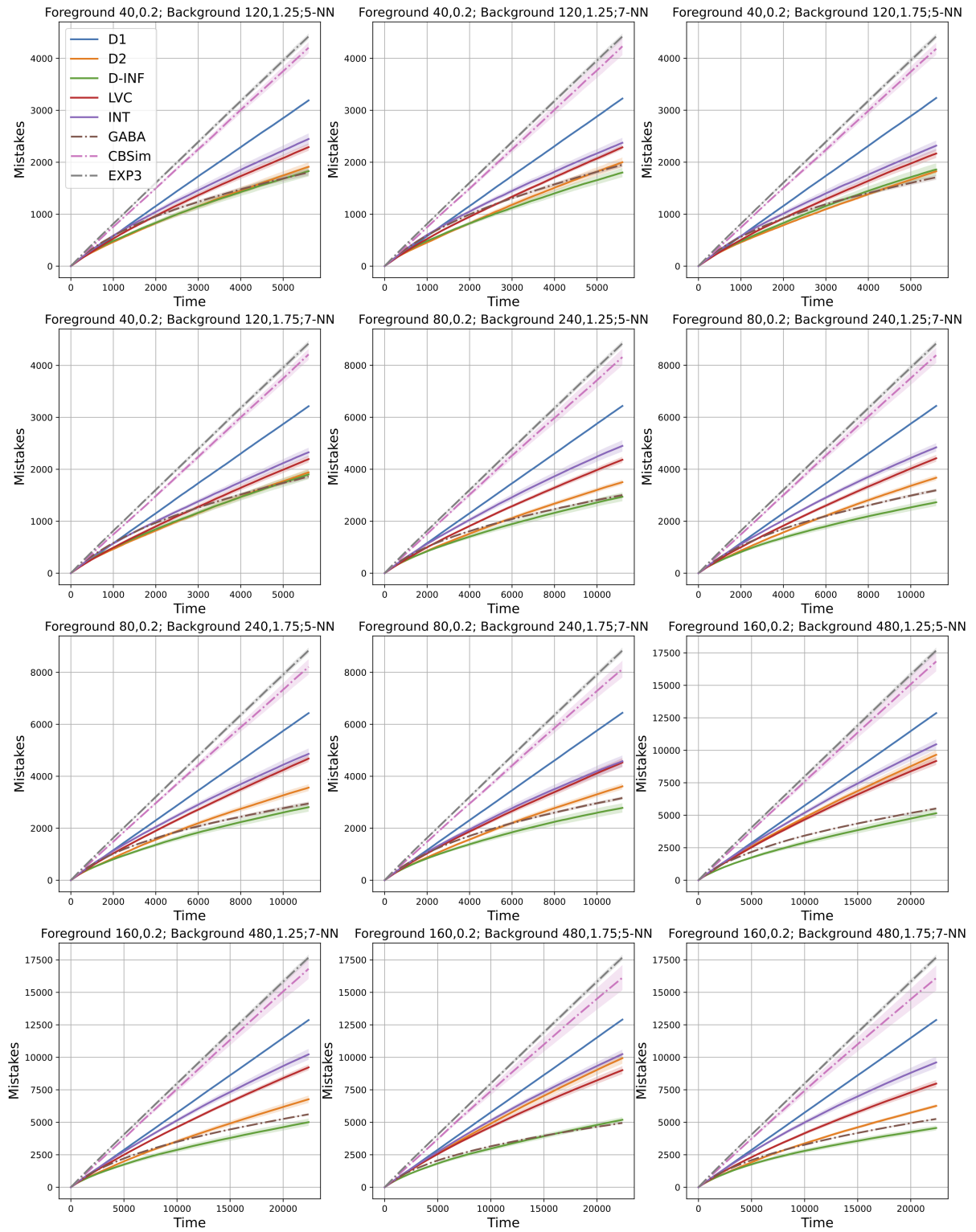


Figure 3. Gaussian graph results, dotted lines represent different baselines, while solid lines are used to represent various results.

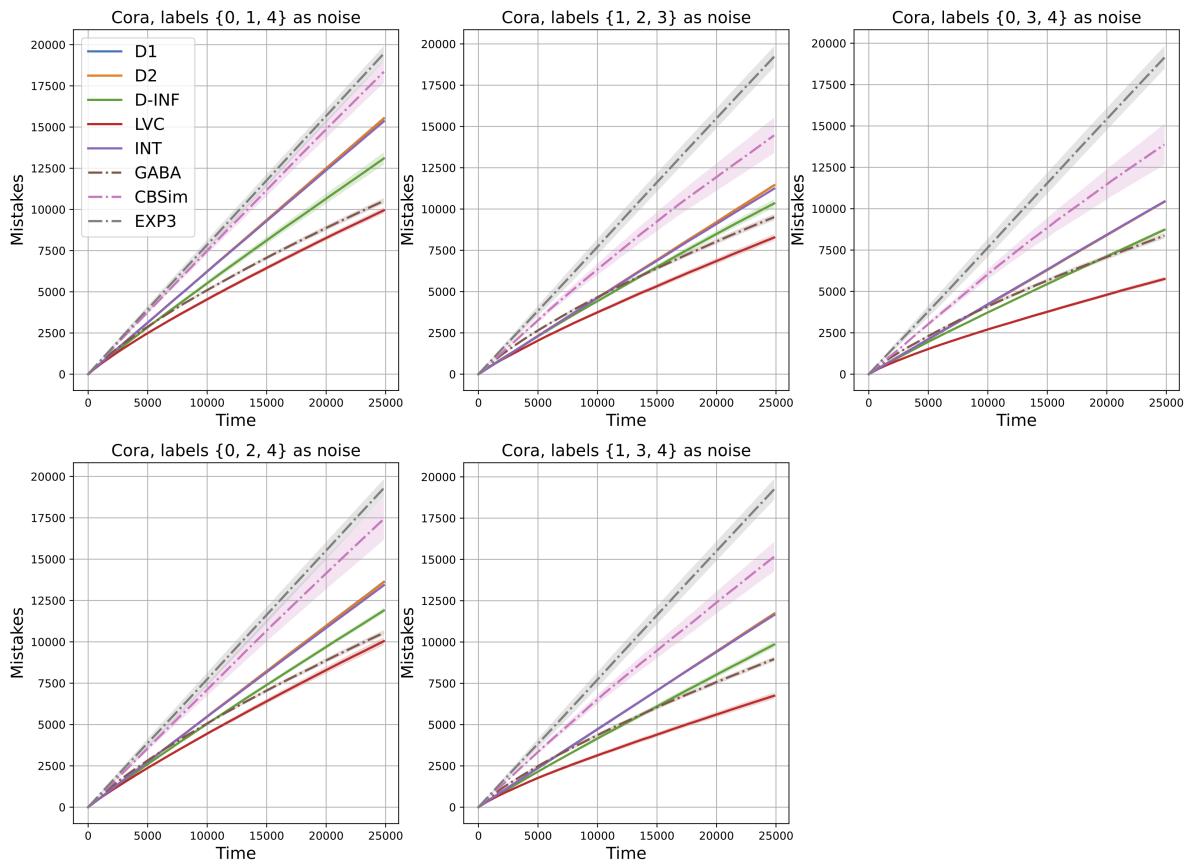


Figure 4. Cora results, dotted lines represent different baselines, while solid lines are used to represent various results



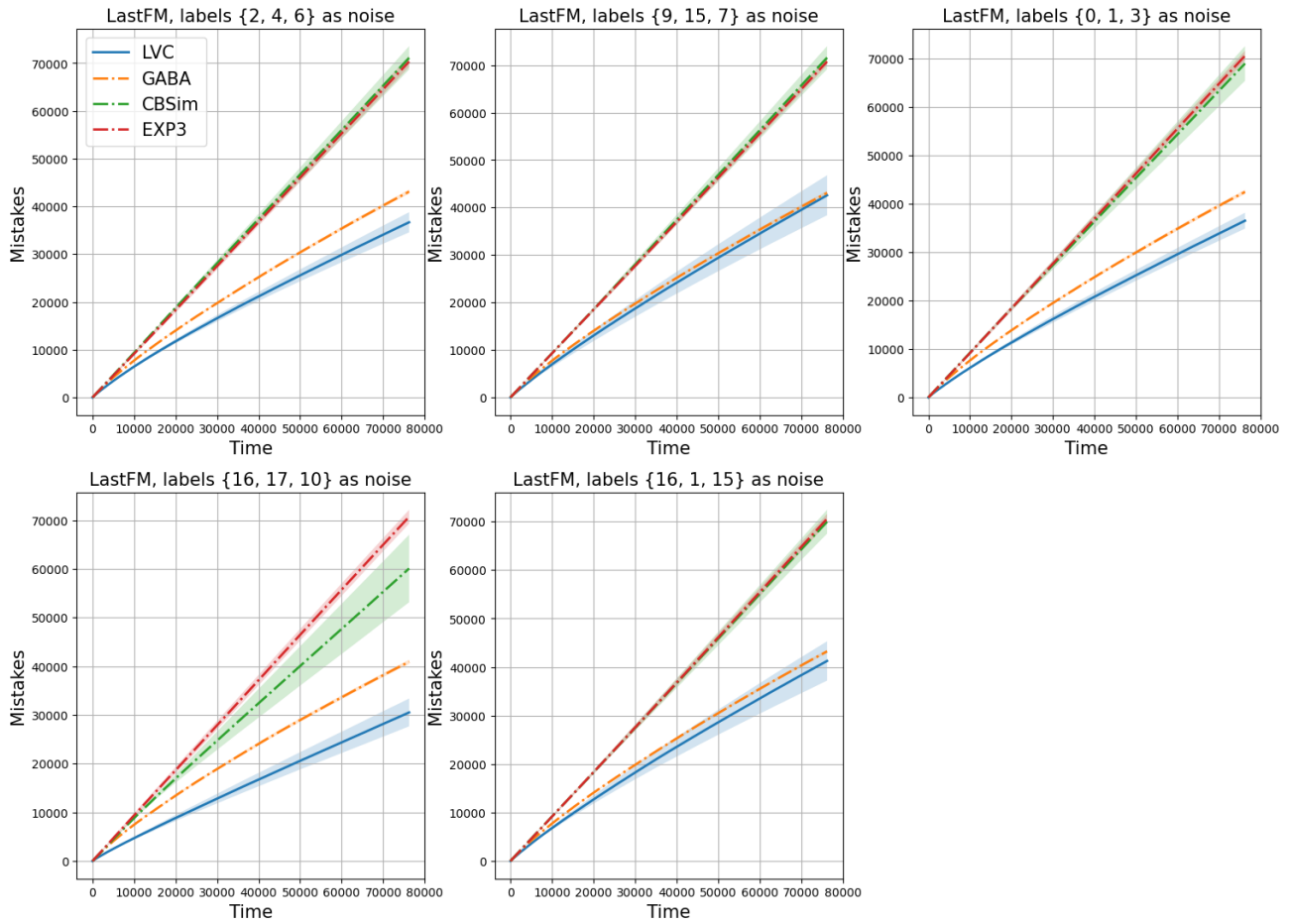


Figure 5. LastFM Asia results, dotted lines represent different baselines, while solid lines are used to represent various results